Supporting Information

Single-Site Cu(II/I) Transition Initiated by Photo-Doping for Enhanced Hydrogenation Activity

Qilong Liu [a], Jixian Wang [a], Qin Liu[b], and Wentuan Bi [a]**

a. Institute of Energy, Hefei Comprehensive National Science Center (Anhui Energy Laboratory), Hefei, Anhui, 230031, P. R. China.

b. State Key Laboratory of Precision and Intelligent Chemistry, University of Science and Technology of China, Hefei, 230026, P. R. China.

E-mail: bwin@ustc.edu.cn. qin0623@ustc.edu.cn.

Synthesis of single-site Cu-C_3N_4 nanosheets and pure C_3N_4 nanosheets

Typically, 2 g of dicyandiamide, 10 g of NH_4Cl and $CuCl_2$ (0.1 mmol, 0.2 mmol, 0.4 mmol, 0.6 mmol, 0.8 mmol and 1.0 mmol, respectively) were dissolved in 60 ml deionized water and stirred at 80 °C overnight. After the water evaporation, a blue-green mixture powder was obtained. Then, 5 g of mixture powder was placed in a crucible and heated at 550 °C for 2 h at a rate of 5 °C min^{-1}. The resultant yellow materials were characterized as single-site Cu-C_3N_4 nanosheets. Pure C_3N_4 nanosheets were obtained under the same reaction conditions without $CuCl_2$ in reactants.

Catalytic hydrogenation measurement

The photocatalytic reaction was carried out in a cylindrical quartz reactor with 2.5 cm inner diameter and 4.5 cm length. A 300 W xenon lamp was used as illuminating source. In detail, 20 mg photocatalyst was dispersed in 2 mL 4-NP aqueous solution (1 mM) by ultrasonic dispersion. Next 2 mL sodium borohydride aqueous solution (0.1 M) was injected into the reactor rapidly. Then the solution was irradiated from the bottom of the reactor. The concentration of 4-NP (after the removal of photocatalysts through centrifugation) was recorded by the UV–Vis spectrophotometer. Wavelength-dependent hydrogenation activity was measured under illumination of light with different wavelengths at normalized intensity (100 mW/cm^{-2}). Since the extremely high concentration of $NaBH_4$ in comparison with that of 4-NP, pseudo-first-order kinetics was generally applied to evaluate the rate constants (k): $\ln(C_o/C_t)=kt$.[1] C_t and C_0 represent the concentration of 4-NP at time t and the initial concentration, respectively.

Characterization methods

The samples were characterized by X-ray powder diffraction (XRD) using a Philips X'Pert Pro Super diffractometer equipped with graphite-monochromatized Cu-Kα radiation (λ =

1.54178 Å). Transmission electron microscopy (TEM) images were taken on H-7650 (Hitachi, Japan) operated at an acceleration voltage of 100 kV. The high-angle annular dark-field scanning transmission electron microscopy (HAADF-STEM) characterization was performed on JEM-ARF200F with a spherical aberration corrector. UV–Vis absorption spectra were recorded on a Perkin Elmer Lambda 950 spectrophotometer. Photoluminescence (PL) emission spectra were obtained on a FLUOROLOG-3-TAU fluorescence spectrometer (Horiba). Electron spin resonance (ESR) spectra were collected at room temperature using a JES-FA200 spectrometer with the microwave frequency of 9.055 GHz. The irradiation experiments were carried out with a xenon lamp (500 W, USHIO Optical Modulex SX-U1501XQ). The copper (Cu) metallic content was quantified using an inductively coupled plasma atomic emission spectrometer (ICP-AES, Model iCAP PRO). Specifically, an accurately weighed 1 mg aliquot of the sample was digested with aqua regia, and the resulting mixture was subsequently diluted to a final volume of 50 mL with distilled water to yield a colorless, transparent solution. A blank control was prepared following the identical protocol, with the sole exception of omitting the sample. In situ XPS measurements were performed on a Shimadzu Kratos Axis Supra+ spectrometer.

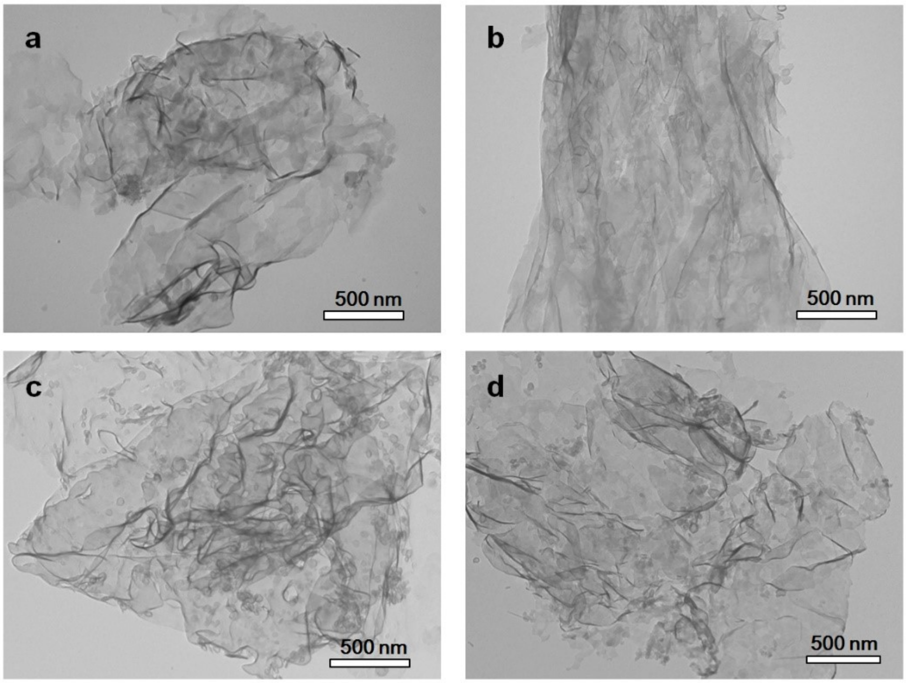

Figure S1. TEM images of Cu-C_3N_4 nanosheets synthesized from precursors with varied molar ratios of Cu/dicyandiamide. (a) 0.84 mol %, (b) 1.68 mol%, (c) 2.52 mol%, (d) 4.2 mol%.

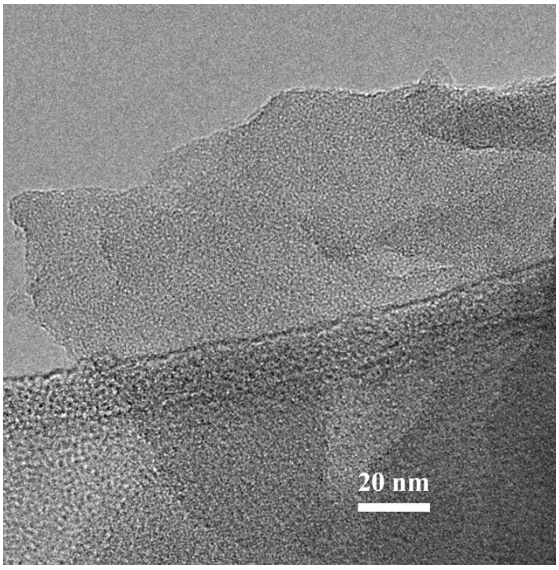

Figure S2 TEM image of Cu-C_3N_4 with Cu radio of 1.6 wt%.

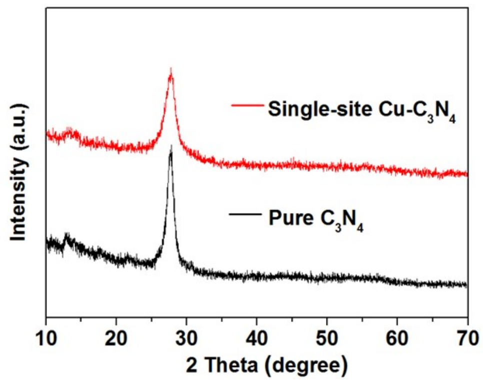

Figure S3. XRD patterns for pure C_3N_4 nanosheets and single-site Cu-C_3N_4 nanosheets (~1.6 wt % Cu).

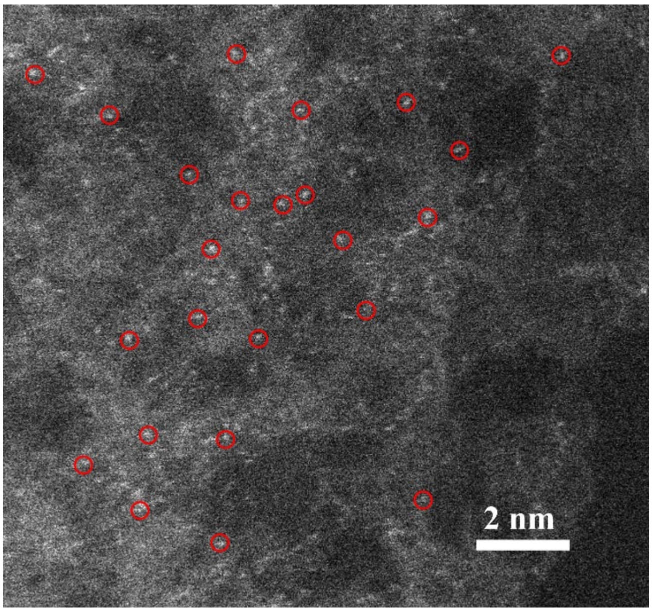

Figure S4 The HAADF-STEM image of Cu-C_3N_4.

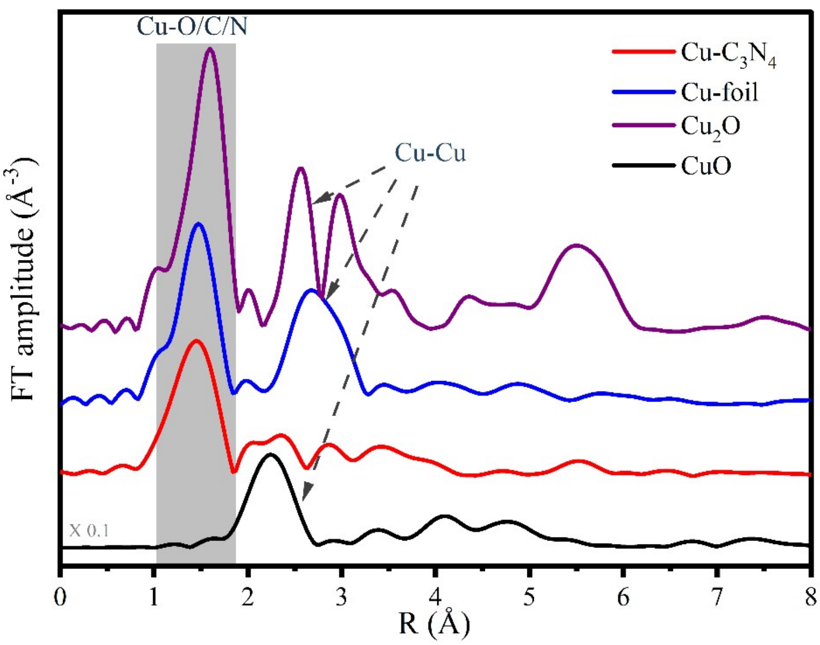

Figure S5 Fourier transforms of the Cu K-edge EXAFS oscillations of single-site Cu-C_3N_4, CuO, Cu_2O and Cu foil.

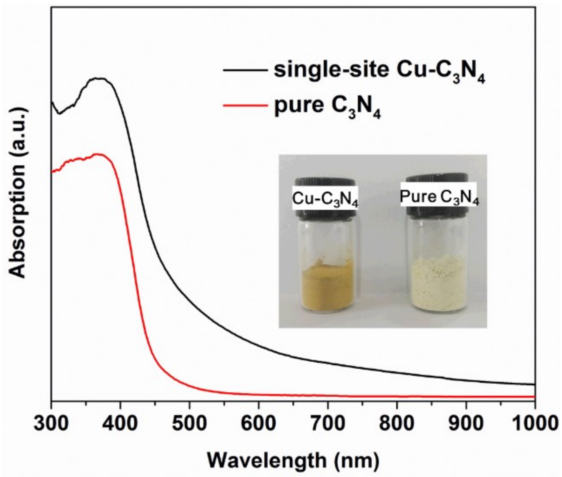

Figure S6. UV−vis absorption spectra of pure C_3N_4 and single-site Cu-C_3N_4. Inset is the corresponding digital photograph.

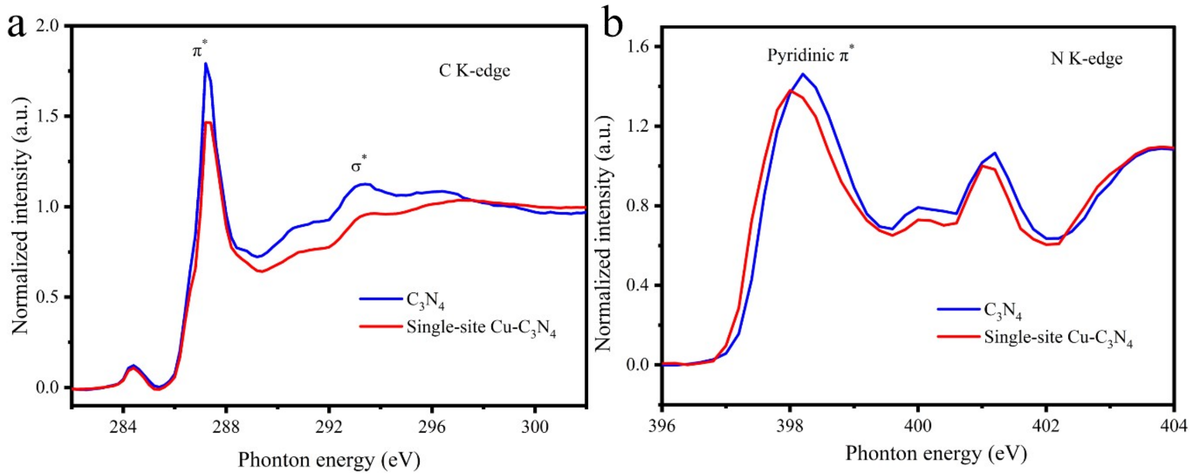

Figure S7 (a) C K-edge and (b) N K-edge X-ray absorption spectra between pure C_3N_4 and single-site Cu-C_3N_4.

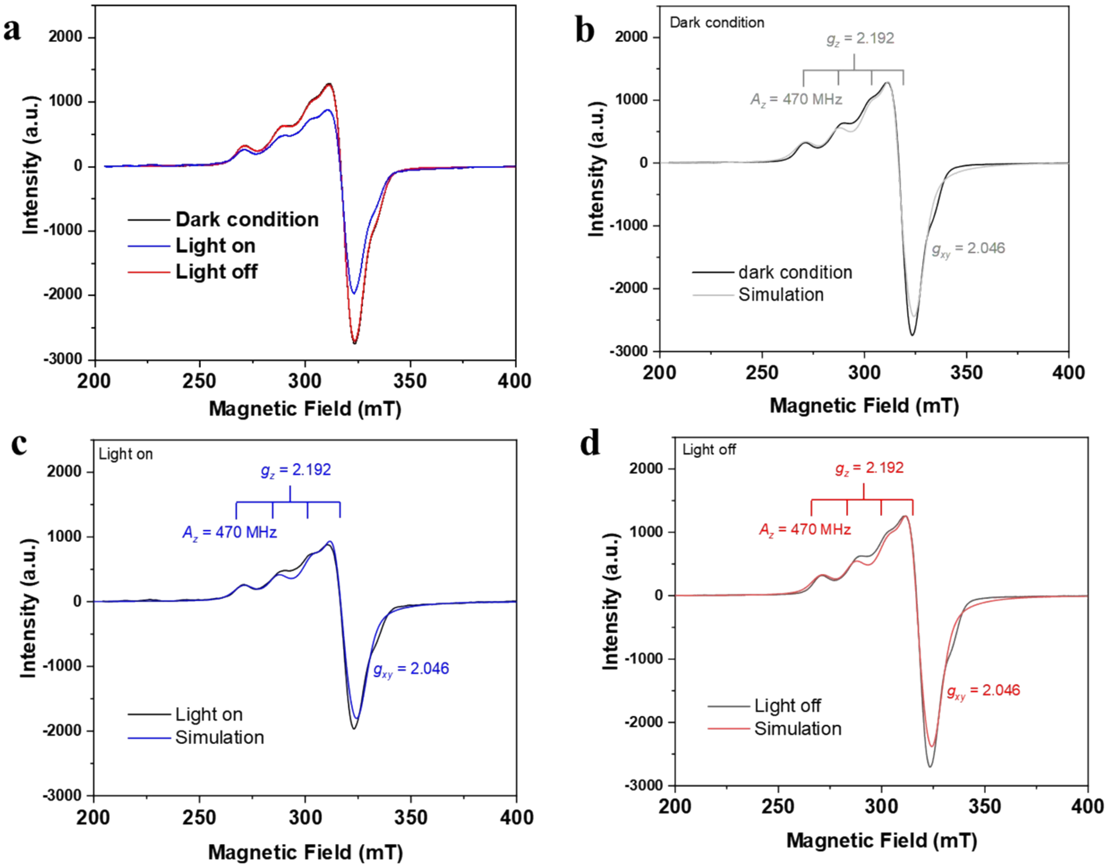

Figure S8 The theoretical modelling of EPR spectra in Cu-C_3N_4 under dark, Light on, and Light off conditions.

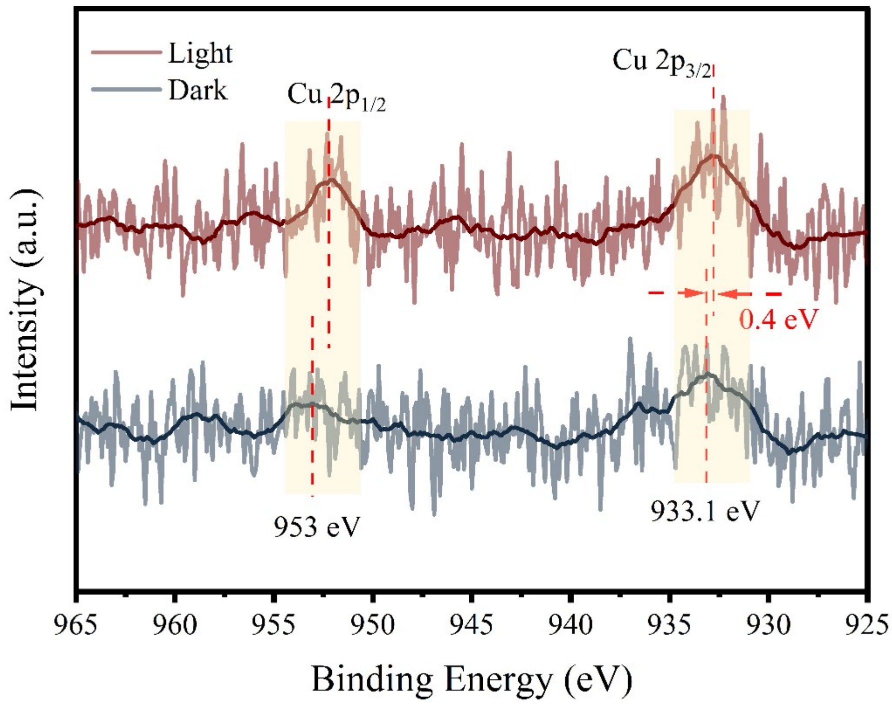

Figure S9 High-resolution XPS spectra of Cu 2p under light irradiation and dark conditions.

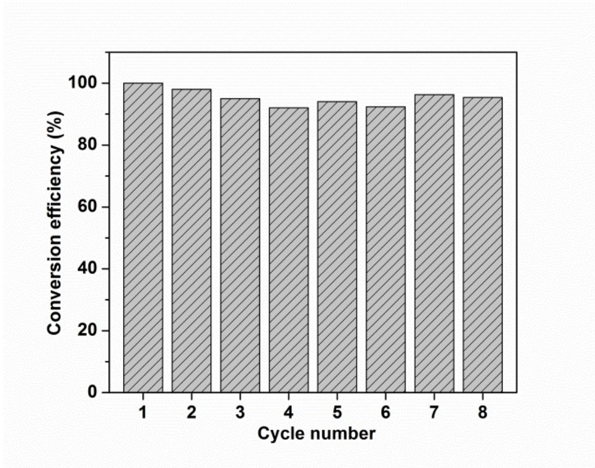

Figure S10. Comparison of conversion efficiency of single-site Cu-C_3N_4 during eight consecutive cycles.

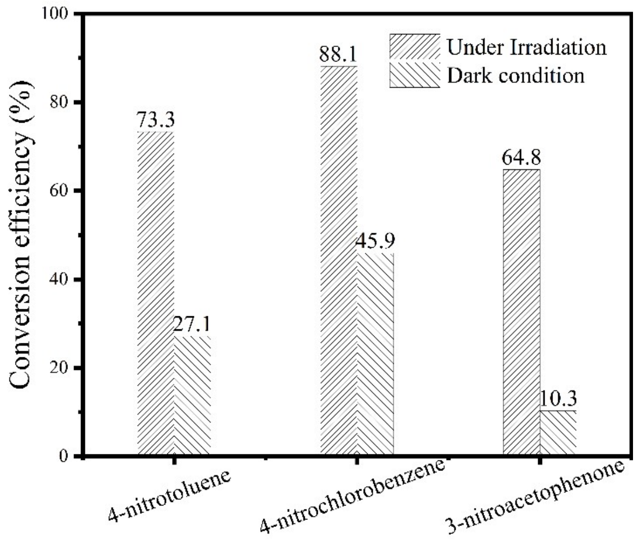

Figure S11 The catalysis performance of other organic hydrogenation reactions.

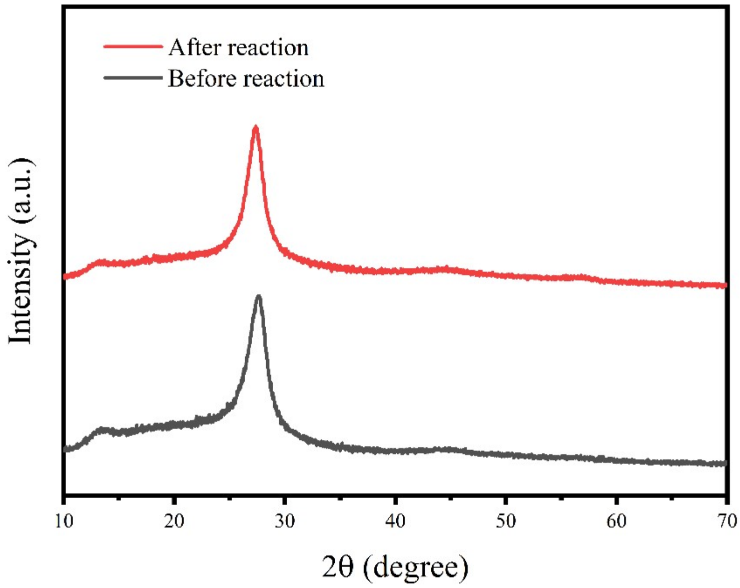

Figure S12 The XRD pattern of Cu-C_3N_4 before and after the reaction.

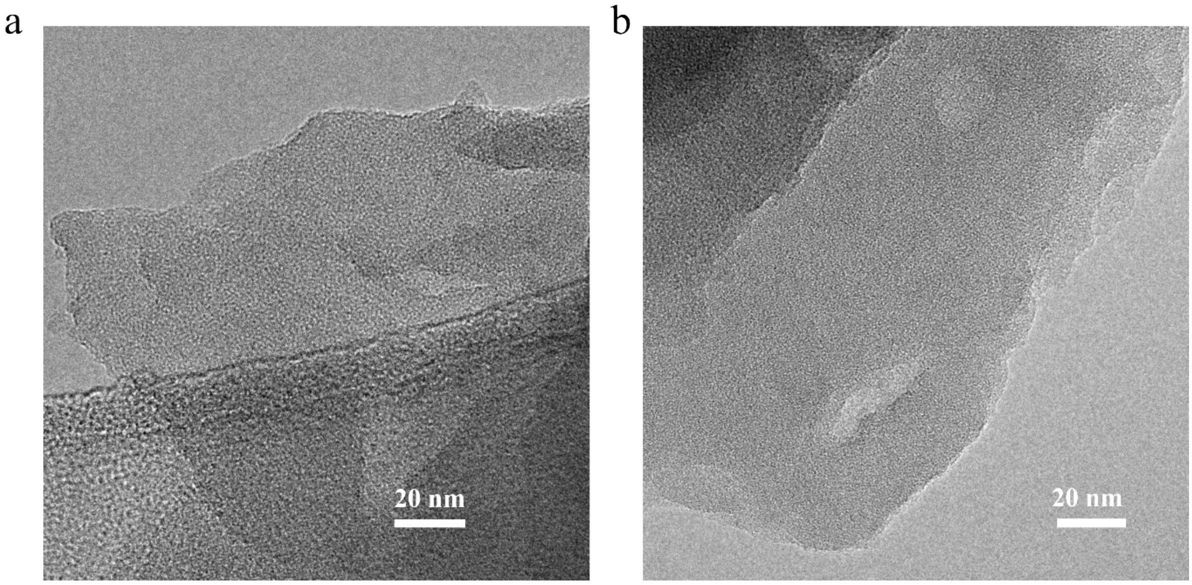

Figure S13 TEM images of Cu-C_3N_4 (a) before and (b) after the reaction.

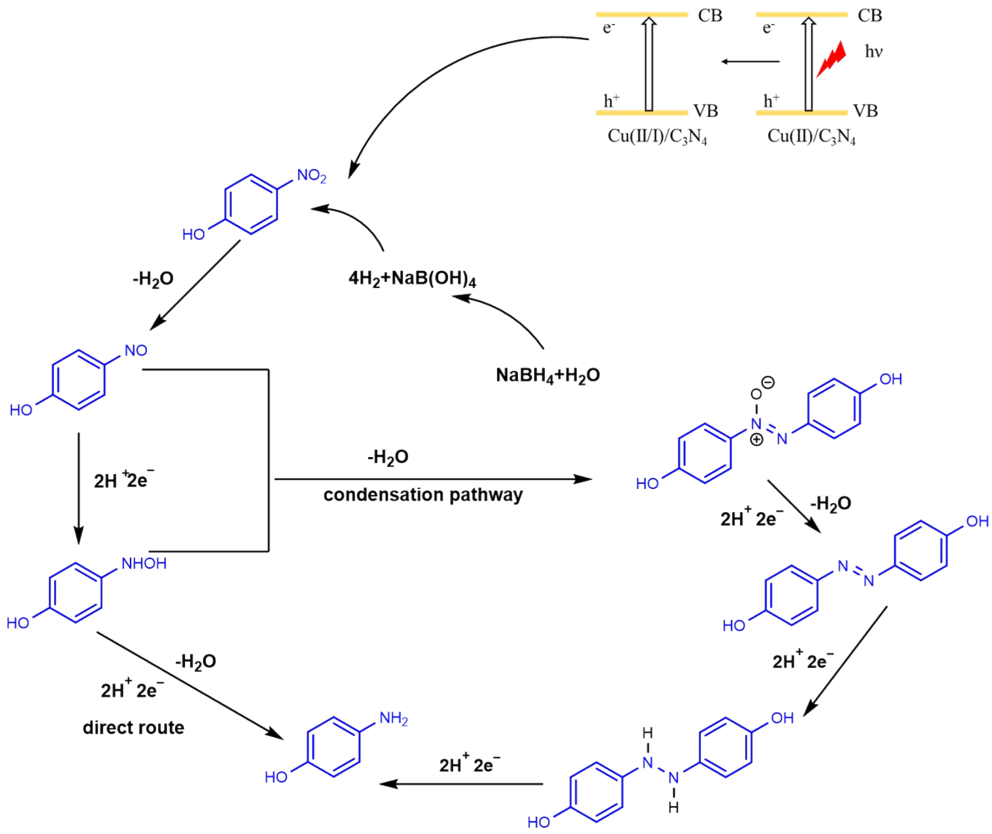

Figure S14 A possible mechanism of the Cu-C_3N_4 photocatalyst under irradiation.

References

[1] J. Ge, Q. Zhang, T. Zhang, Y. Yin, *Angew. Chem. Int. Ed.* **2008**, *47*, 8924.